

Inhibition of insulin-like growth factor I receptor autophosphorylation by novel 6-5 ring-fused compounds

Wanqing Li^a, Svetlana Favelyukis^a, Jie Yang^b, Yibin Zeng^b, Jamming Yu^b,
Aleem Gangjee^b, W. Todd Miller^{a,*}

^aDepartment of Physiology and Biophysics, School of Medicine, State University of New York at Stony Brook,
Basic Science Tower T-6, Stony Brook, NY 11794-8661, USA

^bDivision of Medicinal Chemistry, Graduate School of Pharmaceutical Sciences, Duquesne University, Pittsburgh, PA 15282, USA

Received 3 November 2003; accepted 19 March 2004

Abstract

The insulin-like growth factor 1 receptor (IGF1R) plays an important role in cell transformation, and it has emerged as a target for anti-cancer drug design. IGF1R is activated by autophosphorylation at three sites in the enzyme activation loop. We describe here a group of 6-5 ring-fused compounds that are the first reported inhibitors selective for the unphosphorylated (0P) form of IGF1R. These compounds do not significantly inhibit the fully activated, triply phosphorylated (3P) form. IGF1R was produced from baculovirus-infected *Spodoptera frugiperda* (Sf9) cells, and the 0P and 3P forms were purified to homogeneity. We used a continuous spectrophotometric assay to measure inhibition of the 0P and 3P forms. Analysis by native gel electrophoresis confirmed that the step inhibited in the autoactivation process was the transition between the 0P and IP forms of IGF1R. The compounds were also active against IGF1R autophosphorylation in intact Chinese hamster ovary (CHO) cells. Most of the compounds also inhibited the closely related insulin receptor to varying degrees, although some compounds showed selectivity for IGF1R or insulin receptor. This class of compounds could form the basis of design efforts to selectively block the autoinhibited conformation of IGF1R.

© 2004 Elsevier Inc. All rights reserved.

Keywords: Insulin-like growth factor 1 receptor (IGF1R); Autophosphorylation; Receptor tyrosine kinase

1. Introduction

The insulin-like growth factor-1 receptor (IGF1R) belongs to the superfamily of receptor tyrosine kinases (RTKs) [1,2]. It is widely expressed in many human tissues and cell types [3,4]. IGF1R plays a very important role in cell survival, cell growth and differentiation [4–6]. The IGF1 receptor is involved in both metabolic and survival signaling pathways, which include intermediate proteins such as phosphatidylinositol 3-kinase (PI-3K), the serine/threonine kinase Akt, and GSK-3, PKC and PTP-1B [6]. IGF1R can also induce mitogenesis and promote survival of cells against a variety of apoptotic agents [5]. Studies in knockout mice demonstrate that disruption of the IGF1R can lead to fetal growth retardation and abnormalities in the development of muscle, skin, bone and the central nervous system [7].

The IGF1 receptor plays a role in malignant transformation [8–10]. Overexpression of IGF1R in NIH3T3 cells leads to ligand-dependent morphological transformation [11]. IGF1R is overexpressed in many forms of human cancer, including lung cancer, colon carcinoma, tumors of the CNS, cervical cancer, and Wilms tumor, leading to increased IGF1 signaling in these tumors [8,10]. The survival of these tumor cells is partially dependent on the anti-apoptotic effects of IGF1R. In breast cancer models that overexpress HER2/Neu, increased levels of IGF1R interfere with the action of the HER2/Neu inhibitor Herceptin [12]. Interference with IGF1R (by anti-sense strategies, antibodies, or dominant negative mutants) in a variety of tumor cell lines reverses the transformed phenotype [5]. Inhibition of IGF1R can induce apoptosis in tumor cells by repressing tumor genesis and metastases [5]. Therefore, IGF1R has emerged as a promising target for anti-cancer therapy.

IGF1R belongs to the same RTK subfamily as the insulin receptor (IR) and insulin-related receptor (IRR). IGF1R

* Corresponding author. Tel.: +1-631-444-3533; fax: +1-631-444-3432.
E-mail address: todd.miller@stonybrook.edu (W.T. Miller).

and IR share 70% sequence identity [1]. These receptors consist of two extracellular α -subunits and two transmembrane β -subunits. The tyrosine kinase domains are in the cytoplasmic portions of the β -subunits. Ligand binding to the α -subunit leads to conformational changes in the β -subunits, leading to autophosphorylation of Tyr1131, Tyr1135, and Tyr1136 [13,14]. As explained in detail below, this autophosphorylation is required for full enzyme activity. We refer to the unphosphorylated, mono-phosphorylated, bis-phosphorylated, and tris-phosphorylated forms of IGF1R as 0P, 1P, 2P, and 3P, respectively.

The three-dimensional structures of the 0P, 2P, and 3P forms of IGF1R have been determined [15–17], and the structures of the 0P and 3P forms of insulin receptor have been determined [18,19]. The overall structures of IGF1R and IR are typical of tyrosine kinase domains. They are composed of two major subdomains: an N-terminal lobe, consisting of 5 anti-parallel β -strands and a single α helix, and a C-terminal lobe, consisting of eight α helices and three pairs of anti-parallel β -strands. The autophosphorylation sites Y1131, Y1135, and Y1136 are in the activation loop (A-loop), a mobile segment between the N- and C-terminal lobes.

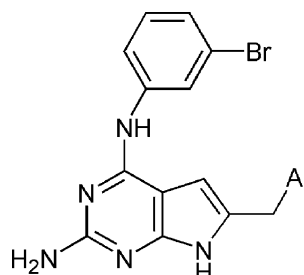
The crystal structure of IGF1RK-3P [17] shows that the ATP is situated in the cleft between the two lobes and peptide substrate binds to the C-terminal lobe, with the phosphate-acceptor tyrosine hydrogen-bonded to conserved residues in the catalytic loop (a segment in the C-terminal that contains catalytic residues). The phosphorylated A-loop is well ordered and anchored to the C-terminal lobe in a conformation that facilitates substrate binding and catalysis. By comparison with the structure of IGF1R0P [15], it is clear that autophosphorylation causes a conformational change in the A-loop, allowing for the binding of ATP and peptide substrate to the catalytic site. Thus, autophosphorylation of IGF1RK and insulin receptor kinase (IRK) is the crucial regulator of the catalytic activity.

As described above, Y1131, Y1135, and Y1136 are the critical autophosphorylation sites for controlling IGF1R activity. The corresponding residues in IR are Y1158, Y1162 and Y1163 [20–23]. Two-dimensional mapping studies revealed that the first residue to be phosphorylated is Y1135, followed by Y1131 and then Y1136 [17]. In the unphosphorylated forms of IGF1RK or IRK, the A-loop adopts an autoinhibitory conformation with Tyr1135 bound in the active site. When the first phosphorylation event occurs in the A-loop, it disrupts the autoinhibited conformation of the β -subunit. Further autophosphorylation of residues Tyr1131 and Tyr1136 in IGF1R stabilizes the catalytically competent enzyme and enhances the enzyme activity [17]. Steady-state kinetic analyses of the isolated phospho-forms of the IGF1RK revealed that each autophosphorylation event increases enzyme turnover number and decreases K_m for ATP and peptide substrates [17].

Although there is wide interest in developing inhibitors to IGF1R, relatively few small-molecule IGF1R inhibitors have been reported. The previously reported IGF1R inhibitors are the tyrphostin-type compounds AG1024, AG1034, and AG538 [24,25]. AG1024 and AG1034 inhibited hormone-stimulated cell proliferation and receptor kinase activity with IC_{50} values in the low micromolar range [25]. AG538 inhibited IGF1R autophosphorylation in intact cells and was reported to be competitive with respect to poly(Glu, Tyr) substrate, rather than with ATP [24]. However, these compounds were not tested on the purified IGF1R, so it was not possible to characterize which of the various phospho-forms of IGF1R were targeted. Here, we report on new classes of IGF1R inhibitors that are selective for the unphosphorylated (0P) form.

Compounds 1–11 (Table 1) were designed as 6-5 ring systems which fit into the general pharmacophore model of RTKs [26,27]. Though 6-5 ring systems such as pyrazolopyrimidines and pyrrolopyrimidines have been reported as RTK inhibitors, to our knowledge, 2-amino substituted pyrrolopyrimidines have not been explored to any significant extent. The rationale for inclusion of a 2-amino moiety in our analogs was that it provides a third H-bonding moiety to the Hinge region of RTKs. The first and second H-bonding groups arise from the amino group of the 4-anilino moiety and the N1 of the pyrimidine ring [26,27]. Thus, using the 4-*m*-bromo aniline, which binds in the hydrophobic region 1 of the general pharmacophore model, and the 2-amino group as in variable groups, we were interested in determining if variations in the

Table 1
Inhibition of IGF1RK and IRK autophosphorylation by 2-amino-4-anilino-6-phenylmethyl pyrrolo[2,3-*d*]pyrimidines

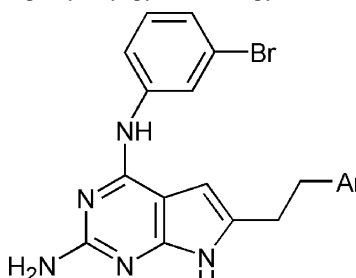


Compounds	Ar	IC_{50} for IGF1RK0P (μ M)	IC_{50} for IRK0P (μ M)
1	4-Cl-Phenyl	10.1	>20
2	2-Cl-Phenyl	7.4	>20
3	1-Naphthyl	>20	>20
4	3,4-diCl-Phenyl	>20	>20
5	4-Biphenyl	>20	2.1
6	Phenyl	6.1	>20
7	2-Naphthyl	>20	>20
8	<i>o</i> -Methylphenyl	>20	6.1
9	2,4-diCl-Phenyl	13.3	>20
10	3,4,5-triOMe-Phenyl	12.6	>20
11	2,5-diOMe-Phenyl	5.1	4.6

Compounds that gave less than 40% inhibition in the initial screening at 20 μ M are listed as $IC_{50} > 20 \mu$ M.

Table 2

Inhibition of IGF1RK and IRK autophosphorylation by 2-amino-4-anilino-6-phenylethyl pyrrolo[2,3-*d*]pyrimidines



The chemical structure shows a pyrrolo[2,3-*d*]pyrimidine core. At position 2, there is an amino group (H₂N). At position 4, there is an anilino group (NH-Ph). At position 6, there is a phenylethyl group (-CH₂-CH₂-Ar). The Ar group is defined in the table below.

Compounds	Ar	IC ₅₀ for IGF1RK0P (μM)	IC ₅₀ IRK0P (μM)
12	1-Naphthyl	>20	>20
13	Phenyl	>20	>20
14	4-OMe-Phenyl	>20	>20
15	2-Cl-Phenyl	>20	>20
16	Pyridinyl	>20	6.7

Compounds that gave less than 40% inhibition in the initial screening at 20 μM are listed as IC₅₀ > 20.

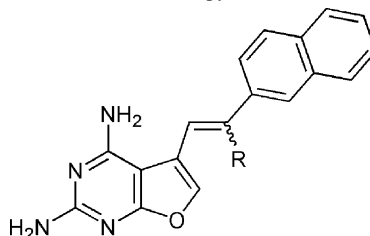
6-substituents of the pyrrolo[2,3-*d*]pyrimidine would afford different selectivities and/or potencies against IRK and IGF1R. compounds **12–16** (Table 2) are two carbon homologs of some of the **1–11** analogs.

An additional facet of the 2-amino-4(*m*-bromoanilino)-6-substituted pyrrolo[2,3-*d*]pyrimidines is that the molecule can bind to the general pharmacophore model in two different binding modes shown in Fig. 1. In mode 1 the molecule binds similarly to ATP. Rotation of 180° about the 2-amino-C2 bond provides mode 2. In this alternate mode 2, the pyrrole N7H mimics the 4-anilino NH of mode 1. In the absence of any crystal structures of pyrrolo[2,3-*d*]pyrimidines with any RTKs, it is not possible to predict which binding mode our analogs **1–17** adopt when bound to IGF1R or to IRK. It is possible that both modes are used and may determine selectivities of the molecules for different RTKs. The rationales for analogs **1–11** have recently been described in detail, along with selected RTK inhibitory activities [28].

Compounds **17–19** (Table 3) are 2,4-diamino-5-substituted furo[2,3-*d*]pyrimidines. These analogs were designed as single agents with both dihydrofolate reductase (DHFR) and RTK inhibitory capabilities. The premise behind this

Table 3

Inhibition of IGF1RK and IRK autophosphorylation by 5-substituted 2,4-diaminofuro[2,3-*d*]pyrimidines



The chemical structure shows a furo[2,3-*d*]pyrimidine core. At positions 2 and 4, there are amino groups (H₂N). At position 5, there is a substituent R. The R group is defined in the table below.

Compounds	R	IC ₅₀ for IGF1RK0P (μM)	IC ₅₀ IRK0P (μM)
17	Methyl (<i>E/Z</i> 2:1)	7.4	6.9
18	H (<i>cis</i>)	7.6	20
19	H (<i>trans</i>)	>20	>20

Compounds that gave less than 40% inhibition in the initial screening at 20 μM are listed as IC₅₀ > 20 μM.

combination comes from the problem that anti-angiogenic agents when used as anti-tumor agents are cytostatic and are unable to eradicate the tumor. It is recommended that some anti-angiogenic agents be used in combination with standard chemotherapeutic agents that are cytotoxic for better therapeutic response. Thus, agents such as **17–19** were expected to combine both the cytostatic (RTK inhibitory activity) along with cytotoxic activity (DHFR inhibition). The details of the design and RTK and DHFR inhibitory activities of these analogs have recently been described [29]. In view of the importance of IGF1R in cancer and a dearth of suitable inhibitors, it was of interest to evaluate analogs **1–19** as inhibitors of IGF1R.

2. Materials and methods

2.1. Expression and purification of IGF1RK

We expressed and purified IGF1R kinase domain essentially as described [17]. We infected *Spodoptera frugiperda* (Sf9) cells with a recombinant baculovirus encoding residues 956–1256 of the human IGF1R. Cells were harvested after 72 h infection and lysed in a French pressure cell in lysate buffer containing 20 mM Tris-HCl, pH 7.5, 5 mM EDTA, 2 mM dithiothreitol (DTT), 0.2% (v/v) Triton

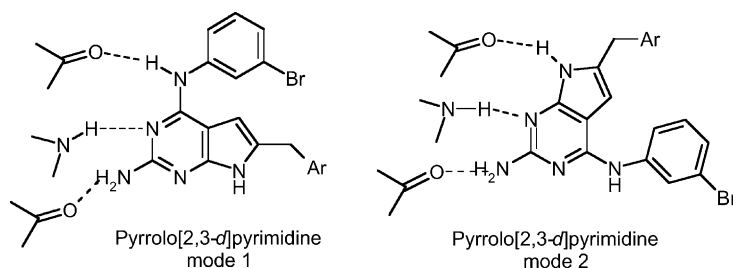


Fig. 1. The two potential modes of binding for 2-amino-4-(*m*-bromoanilino)-6-substituted pyrrolo[2,3-*d*]pyrimidines to the hinge region of the general pharmacophore of receptor tyrosine kinases.

X-100, 5 µg/ml leupeptin, 5 µg/ml aprotinin and 2 mM phenylmethylsulfonyl fluoride. After centrifugation and filtration, IGF1RK0P was purified by three chromatographic steps on FPLC (Amersham Pharmacia Biotech Company). The three columns are: (1) Source-Q 15 ion exchange; (2) Superdex 75 gel filtration; and (3) Mono-Q. To produce IGF1RK 1P, 2P and 3P, the IGF1RK0P was incubated with 10 mM ATP and 30 mM MgCl₂ for 5 min at room temperature. The reaction was terminated by addition of 100 mM EDTA. The reaction mixture was loaded on to Superdex-75 first to remove all the ATP, MgCl₂ and EDTA. Then, the four forms of IGF1RK were separated on a Mono-Q column. Each form of IGF1RK was pooled individually and concentrated.

2.2. Kinase assays and IC₅₀ measurement

A continuous spectrophotometric assay was used to measure the kinase activity of the catalytic domain of IGF1R [17,30]. In this assay, production of ADP is coupled to the oxidation of NADH, which is measured as a decrease in absorbance at 340 nm. The assays were carried out in 100 mM Tris–HCl (pH 7.5), 10 mM MgCl₂, 1 mM phosphoenolpyruvate, 0.28 mM NADH, 89 units/ml pyruvate kinase, 124 units/ml lactate dehydrogenase, 2% DMSO, and at 30 °C in a 50 µl reaction volume. Reactions were initiated by the addition of ATP to mixtures containing enzyme and various concentrations of inhibitors. Assays of IGF1RK-0P autophosphorylation were carried out at 6 µM enzyme and 1 mM ATP. The IGF1RK-3P peptide phosphorylation assays were carried out with 150 nM enzyme, 100 µM ATP, and 500 µM peptide substrate (KKEEEEYMMMM).

2.3. Native gel electrophoresis

Kinase autophosphorylation reactions were carried out with 20 µM enzyme in 20 mM Tris, pH 7.5, 30 mM MgCl₂, 6% DMSO, and 5 mM ATP with or without 50 µM inhibitors at room temperature. Reactions were started by adding ATP, and terminated at varied time points by addition of 100 mM EDTA. The reaction mixtures were separated on 10% Tris–HCl gels under native conditions. The phospho-forms of IGF1R were visualized by colloidal Coomassie blue staining.

2.4. Inhibition of IGF1R autophosphorylation in intact CHO cells

Chinese hamster ovary (CHO) cells overexpressing wild type IGF1 receptors [31] were cultured in DMEM supplemented with 10% dialyzed FBS, 100 µM non essential amino acids, 1% L-glutamine, 1% antibiotic and antimycotic solution, 500 µg/ml geneticin, and 2 µM methotrexate in a humidified atmosphere of 95% air and 5% CO₂ at 37 °C. Confluent cells in 60 mm plates were incubated

overnight with serum-free (SF) medium (HAM F-12, 0.5% sterile BSA, and 1% antibiotic and anti-mycotic). The inhibitors were added at various concentrations in fresh SF medium for 1 h. Cells were then stimulated with 10 nM IGF1 for 1 min. After treatment, cells were washed twice with ice-cold PBS, harvested, and lysed with fresh lysis buffer (25 mM Tris, pH 8.0, 2 mM EDTA pH 8.0, 140 mM NaCl, 1% NP-40, 10 µg/ml aprotinin, 20 µM phenylmethylsulfonyl fluoride (PMSF), 10 µg/ml leupeptin and 10 mM orthovanadate). Cells were lysed for 1 h at 4 °C, then the lysates were cleared by centrifugation at 14,000 × g for 10 min. Protein concentrations of the post-nuclear supernatants were determined by the Bradford method (Bio-Rad). To measure tyrosine phosphorylation of the β-subunits of the IGF1 receptors, lysates were incubated overnight at 4 °C with 2 µg of anti-IGF1R antibody (C-20, Santa Cruz Biotechnology) and 25 µl of 50% protein-A agarose slurry. After three washes with lysis buffer, pellets were resuspended in SDS–PAGE sample buffer and boiled for 3 min. Proteins were resolved by SDS–PAGE (7.5%) and transferred by electroblotting onto PVDF membrane. Tyrosine phosphorylated receptors were detected by immunoblotting with anti-phosphotyrosine antibody (4G10, Upstate Biotechnology) and then stripped and reprobed with anti-IGF1R antibody. Detection was with the ECL method (Amersham). To ensure that the CHO cells remained viable over the time course of the experiment, cells were harvested after treatment with inhibitors, stained with trypan blue, and counted in a hemocytometer.

3. Results

3.1. Inhibition of IGF1R-0P autophosphorylation

We expressed and purified IGF1R kinase domain (IGF1RK) using a strategy developed previously in our laboratory [17]. This strategy allowed us to isolate the four phospho-forms of IGF1RK (0P, 1P, 2P, 3P); we used 0P and 3P forms for this study. We first developed a screening method to identify inhibitor candidates. We assayed all compounds at a final concentration of 20 µM in an initial screening by performing a coupled spectrophotometric assay (Fig. 2). This assay measures autophosphorylation directly, rather than indirectly via substrate phosphorylation [17]. Because all inhibitor compounds were dissolved and stored in 100% DMSO, and because high concentrations of DMSO affect the kinase assay, we kept the final concentration of DMSO at 5%. For comparison, we used AG538 and AG1024, which are known inhibitors of IGF1RK [24,25]. Several of the compounds blocked enzyme autophosphorylation in this assay, and they were more effective than AG1024 at an equivalent concentration (Fig. 2). Based on the inhibition of IGF1RK-0P autophosphorylation, we chose the eight most effective inhibitors for further inhibition studies.

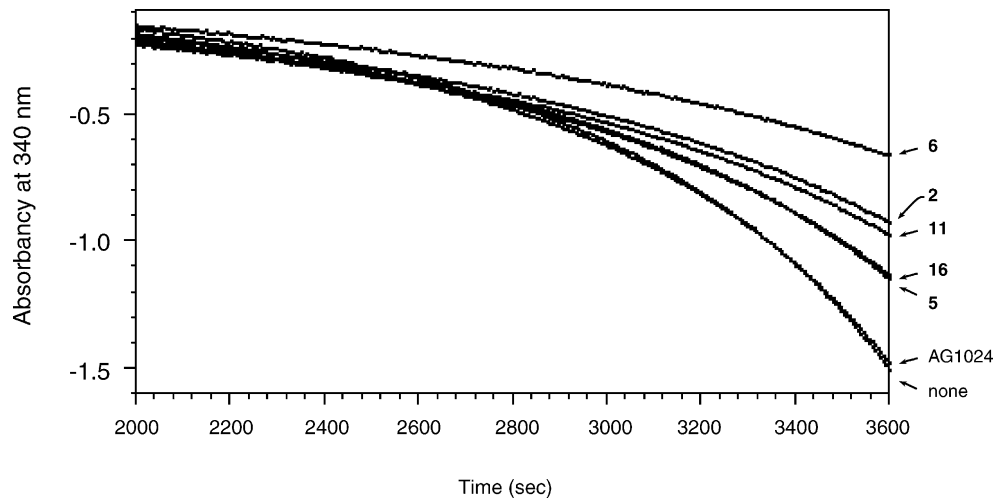


Fig. 2. Screen for inhibition of IGF1RK-0P autophosphorylation. IGF1RK-0P was assayed with the coupled spectrophotometric assay. The inhibitors were present at a concentration of 20 μ M (five representative compounds are shown here). The enzyme concentration was 6 μ M. AG1024, a known inhibitor of IGF1R, was included for comparison. Absorbance measurements were taken every 6 s.

We determined IC_{50} values against IGF1RK autophosphorylation for the best eight inhibitors. To determine IC_{50} , we incubated 6 μ M IGF1RK0P in the presence of 1 mM ATP, 30 mM $MgCl_2$ and varying concentrations of

inhibitor. The rate of autophosphorylation, as visualized by a decrease in slope in the coupled assay, was reduced with increasing inhibitor concentrations (Fig. 3A shows an example for compound **18**). These rates were then used

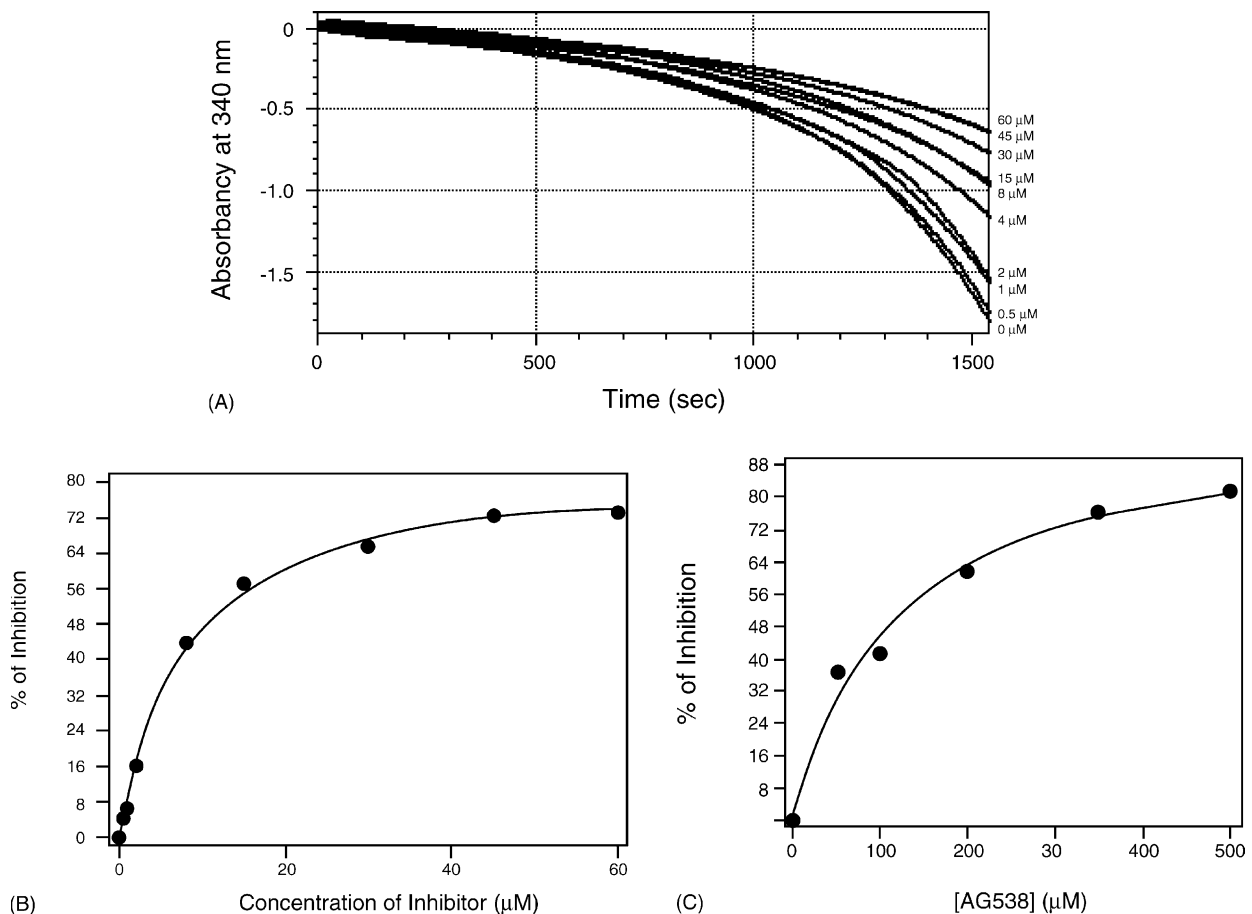


Fig. 3. A representative IC_{50} determination for IGF1RK-0P autophosphorylation. (A) Varying concentrations of compound **18** (shown to the right of the graph) were incubated with IGF1RK-0P. Enzyme activity was measured using the spectrophotometric assay, and the slopes of the enzyme progress curves from 1400 to 1500 s were used to calculate percent inhibition. (B) Plot of percent inhibition vs. [18]. The data were fit to a modified form of the Michaelis–Menton equation to determine IC_{50} s using the program Mac Curve Fit. (C) Similar experiments were carried out with inhibitor AG538 [24].

to calculate the percent of inhibition, and these data were fit to the Michaelis–Menton equation (Fig. 3B). The results confirmed that this series of inhibitors is more potent than AG538 and AG1024. The 6-5 ring-fused inhibitors showed IC_{50} values in the range of 5–15 μ M (Tables 1–3). By comparison, the IC_{50} of AG1024 for inhibition of IGF1RK-OP autophosphorylation in the coupled assay was measured to be 94.2 μ M, and the IC_{50} for AG538 was 114 μ M (Fig. 3C).

A shortcoming of the autophosphorylation assay is that it requires high concentrations of enzyme; IGF1R autophosphorylation is an intermolecular reaction [17], and the rate depends on the concentration of IGF1R-OP used. We use 6 μ M IGF1RK-OP and 2 μ M IRK-OP in our assays, and that prevented us from measuring IC_{50} values in the sub-micromolar level. We were unable to obtain reliable data at lower enzyme concentrations in the spectrophotometric assay. To test whether the inhibitors were effective at lower concentrations, we have attempted several other assays, including anti-phosphotyrosine Western blotting and 32 P-ATP incorporation. However, we found that the rate of the IGF1RK-OP autophosphorylation reaction is very slow below 2 μ M IGF1RK, no matter which assay is used (WQL and WTM, unpublished observations). Thus, our autophosphorylation assay is not suited to measuring sub-micromolar IC_{50} s, and the values we measured could be regarded as an upper limit.

To address the mechanism of inhibition of IGF1RK autophosphorylation, we carried out kinetic studies in the presence of adenosine 5'-(β,γ -imido)triphosphate (APPNHP), a nonhydrolyzable ATP analog. Experiments were carried out with varying concentrations of APPNHP and compound 6. If compound 6 and APPNHP bound in a mutually exclusive fashion to the ATP binding site of IGF1RK, Dixon plots of $1/v$ versus the concentration of compound 6 at different fixed concentrations of APPNHP would yield a family of parallel curves [32]. The results, however, showed that the slopes of these plots were dependent on the concentration of APPNHP (Fig. 4). Thus, APPNHP and compound 6 are nonexclusive inhibitors. These studies suggest that compound 6 is not a pure competitive inhibitor with respect to ATP, but instead that the mode of inhibition is more complex.

3.2. Inhibition of insulin receptor kinase

Insulin receptor shares a high homology sequence with IGF1R, particularly in their kinase domains (84% sequence identity) [1]. To test whether the 6-5 ring-fused inhibitors are specific for IGF1RK-OP, we screened these compounds as inhibitors of insulin receptor kinase domain autophosphorylation. IC_{50} values for IRK are given in Tables 1–3. Not surprisingly, most of the compounds were roughly equally effective against IRK and IGF1RK. However, a few showed a preference for IRK or IGF1RK. For example, compounds 2 and 6 showed a modest preference for

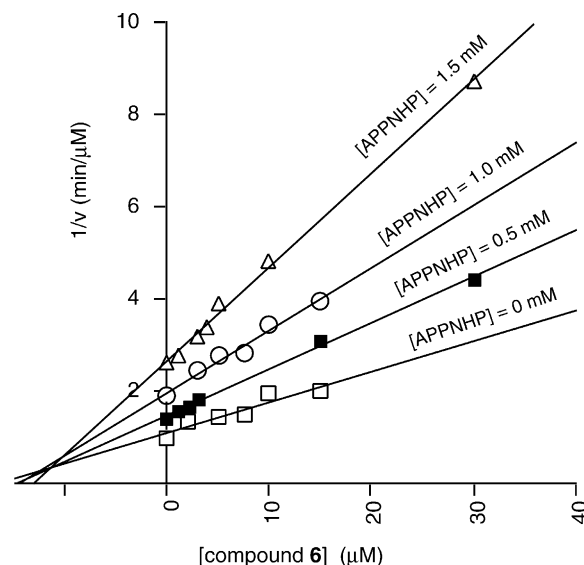


Fig. 4. Inhibition of IGF1RK-OP autophosphorylation by compound 6 in the presence of varying concentrations of APPNHP. Autophosphorylation reactions were analyzed by the coupled spectrophotometric assay, as described in Section 2. The enzyme concentration was 6 and the ATP concentration was fixed at 1 mM.

inhibition of IGF1RK autophosphorylation. Compounds 5, 6, 16, and 18 showed a lower IC_{50} for IRK. In the case of 5, the difference was greater than 10-fold; this was the largest selectivity observed for an inhibitor in this series, and it is among the most selective compounds reported.

3.3. Inhibition of IGF1R-3P substrate phosphorylation

We also checked the effect of the inhibitors on phosphorylation of a peptide substrate by IGF1RK-3P, the fully phosphorylated, active form of IGF1R. In these experiments, carried out with the coupled assay, we incubated 20 μ M inhibitors with 150 nM IGF1RK-3P in the presence of 500 μ M peptide substrate and 100 μ M ATP. The peptide substrate used had the sequence, KKEEEEYMMMM. We previously showed that this peptide is an excellent substrate for IGF1RK, with a K_m value of 120 μ M for the 3P form [17]. The result of our screening showed that none of the inhibitors inhibits IGF1RK-3P (results for several compounds are shown in Fig. 5). Similar results were obtained at concentrations of ATP below K_m (data not shown). AG538 and AG1024, the tyrphostin-type inhibitors, gave a modest degree of IGF1RK-3P inhibition at the same concentration. Even at very high concentrations of AG538 (240 μ M), only a \approx 30% decrease in the enzyme rate was observed (Fig. 5).

3.4. Native gel analysis

To further explore the mechanism of inhibition, we carried out kinase autophosphorylation reactions, stopped the reactions at various time points, and then separated the different phosphorylated forms of enzyme (OP, 1P, 2P,

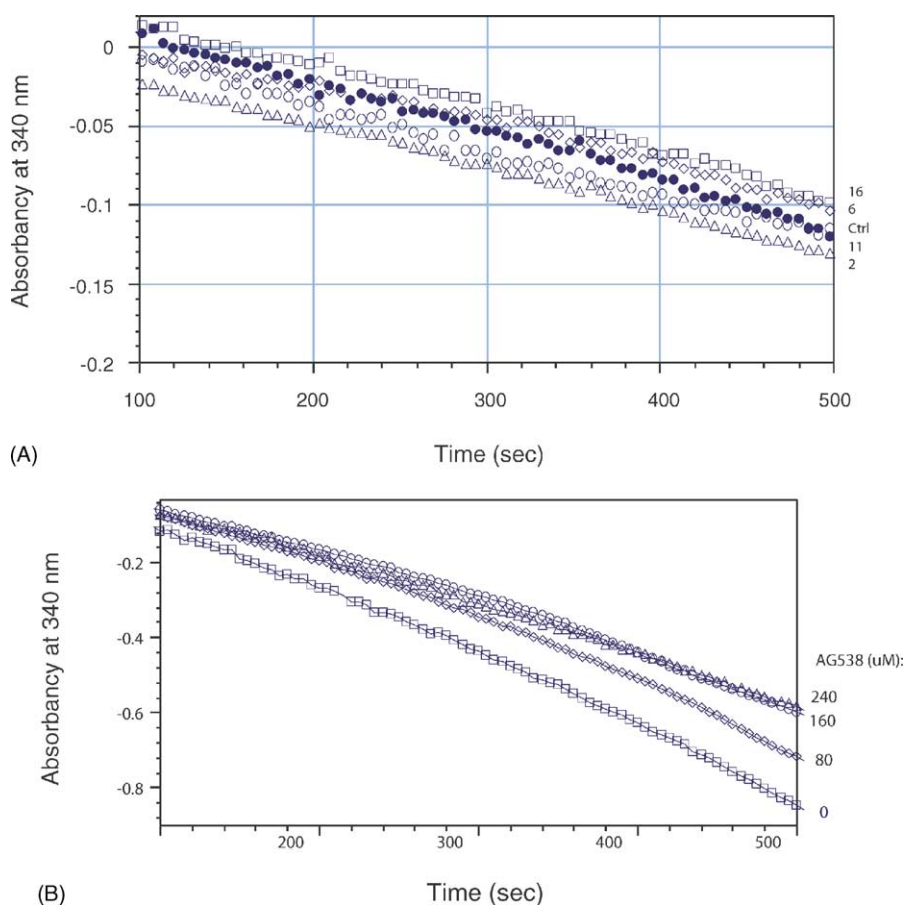


Fig. 5. (A) Screens for inhibition of peptide phosphorylation by IGF1R-3P. Enzymatic activity was measured with the spectrophotometric assay. The enzyme concentration was 150 nM, and the peptide concentration was 500 μM. Inhibitors were present at a concentration of 20 μM. Absorbance measurements were taken every 6 s. Open circles, reaction without inhibitor; squares, reaction with compound **16**; triangles, reaction with compound **2**; diamonds, reaction with compound **6**; closed circles, reaction with compound **11**. The slopes of these enzyme progress curves did not show any significant differences. (B) Similar experiments were carried out with various concentrations of AG538.

and 3P) by 10% PAGE under native conditions (Fig. 6A). Most inhibitors affected the transition from 0P to 1P. Compounds **2** and **6** slowed the rate of autophosphorylation, as compared to control reactions (Fig. 6). AG1024 also showed inhibition similar to compound **2**; however, it was necessary to use a higher concentration (400 μM) to see any effect. These native gel results are consistent with our IC_{50} studies: **6** is a more effective inhibitor than **2**, which is more efficient than AG1024 (The IC_{50} values for **6**, **2**, and AG1024 are: 6.1, 7.4 and 94.2 μM, respectively). AG538 gave no detectable inhibition in this assay (data not shown). We also used the native gel assay to confirm the selectivity of compound **5** for insulin receptor as compared to IGF1R. At a concentration of 100 μM, **5** gave a modest decrease in the rate of IGF1R autophosphorylation, but a similar experiment with insulin receptor resulted in a dramatic blockage of autophosphorylation (Fig. 6B).

3.5. Inhibition of IGF1R autophosphorylation in CHO cells

To test for inhibition of IGF1R autophosphorylation in intact cells, we used Chinese hamster ovary cells stably

overexpressing full-length IGF1R. When grown in the presence of methotrexate, these cells overexpress IGF1R to a level of $>10^7$ molecules per cell [31]. Quiescent CHO/IGF1R cells (16 h serum deprived) were incubated in the presence of various concentrations of compound **2**. These cells were stimulated with 10 nM IGF1 for 1 min at 37 °C and cell lysates were prepared. Control cells were not stimulated with IGF1. Equal amounts of total protein were immunoprecipitated with anti-IGF1R antibody and the immunocomplexes were analyzed by SDS-PAGE, followed by Western blotting with anti-Tyr(P) antibody (4G10). As shown in Fig. 7, IGF1 treatment led to an increase in IGF1R autophosphorylation. In the presence of compound **2**, there was a significant decrease in IGF1-stimulated receptor phosphorylation. The level of IGF1R inhibition in this experiment roughly correlated with the IC_{50} determination made on purified IGF1R-0P (Table 2). The levels of IGF1R protein in immunoprecipitates from the inhibitor-treated and untreated CHO/IGF1R cells were similar, as judged by reprobing the membrane with anti-IGF1R antibody (Fig. 7). The selectivity for IGF1R versus insulin receptor appeared to be retained in intact cells; compound **16** was a more effective inhibitor against CHO

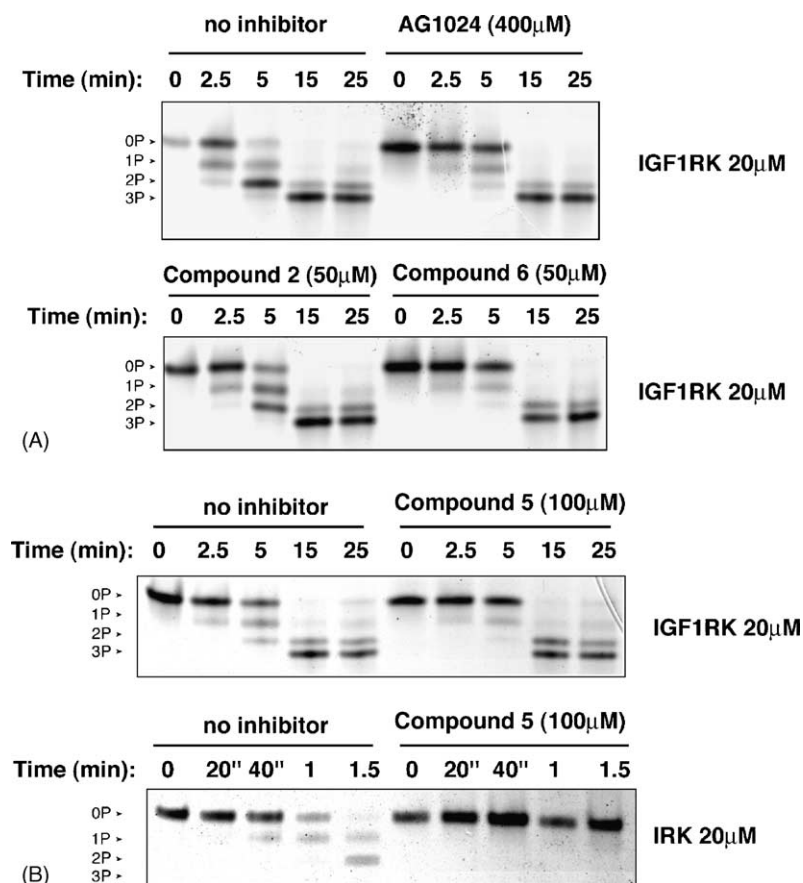


Fig. 6. Native PAGE analysis of the inhibition of IGF1RK-OP and IRK-OP autophosphorylation. Enzymes were present at 20 μM, and the concentrations of inhibitors are indicated. At various time points, reactions were stopped by addition of 100 mM EDTA. The four forms of IGF1RK were then resolved by 10% PAGE and visualized by colloidal Coomassie staining. (A) Inhibition of IGF1RK-OP by compounds **2** and **6** (50 μM) and by AG1024 (400 μM). (B) A comparison of the effect of compound **5** on autophosphorylation of IGF1RK-OP and IRK-OP. Controls without inhibitor contained the same percentage of DMSO (2%) as reactions with inhibitors.

cells overexpressing insulin receptor than against CHO/IGF1R cells (data not shown); this parallels the *in vitro* analysis (Table 2). By trypan blue staining, we confirmed that the cells treated with inhibitor retained viability (cells

were 92% viable after the experiment, in the presence of either inhibitor or a DMSO control). Thus, the 6-5 ring-fused inhibitors studied here have the capacity to interfere with IGF1R autophosphorylation in intact mammalian cells.

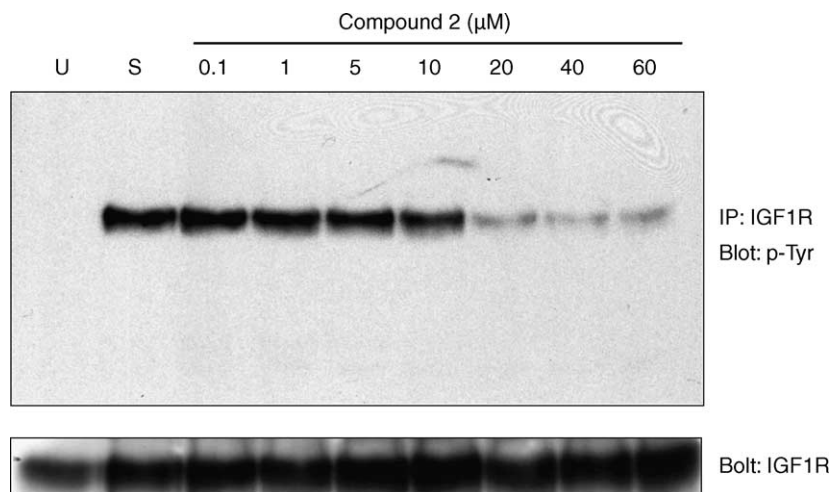


Fig. 7. Inhibition of IGF1R autophosphorylation in CHO cells overexpressing full-length IGF1R. Following overnight starvation, compound **2** was incubated with cells for 1 h. After stimulation with 10 nM IGF1 for one minute, cells were washed, harvested, and lysed. IGF1R was immunoprecipitated and analyzed by SDS-PAGE followed by Western blotting with anti-phosphotyrosine antibody 4G10 (top panel). The same membrane was stripped and reprobed with IGF1R antibody (bottom panel). U: unstimulated cells; S: stimulated cells in the absence of compound **2**.

4. Discussion

We report here the development of IGF1R inhibition assays using the isolated phospho-forms of IGF1RK. Using the spectrophotometric assay (Fig. 3) and the native gel assay (Fig. 6), we have characterized a series of inhibitors that bind to the unphosphorylated IGF1RK0P and prevent the transition to the 1P form. These inhibitors were much less effective against the fully activated, triply phosphorylated form of IGF1RK (Fig. 5). Although we have not attempted to characterize the phosphorylation state of IGF1R in our cell-based assays, it is likely that this represents a mixture of phosphorylated forms. Nonetheless, the inhibitors studied here were able to block ligand-mediated IGF1R autophosphorylation in intact cells (Fig. 7). Although we have not directly measured the cell permeability of these compounds, we note that the compounds studied here have previously been shown to be active in the high nanomolar range against other RTKs in intact cell assays [28,29].

Of the three unique classes of compounds tested here, two classes had compounds that were active against IGF1R autophosphorylation. The first class was the 2-amino-4-anilino-6-phenylmethyl pyrrolo[2,3-*d*]pyrimidines (compounds 1–11; Table 1) that were previously shown to inhibit other receptor tyrosine kinases, including the VEGF, EGF, PDGF, and Flt-1 receptors [28]. Of the various benzyl substitutions at the 6-position of the pyrrolo[2,3-*d*]pyrimidine, the phenyl group (compound 6) and chlorophenyl group (1 and 2) showed better inhibitory characteristics than bulkier substitutions, such as naphthyl (3 and 7), dichloro (4), biphenyl (5), or methylphenyl (8) (Table 1). This general trend for IGF1R autophosphorylation was also observed for other RTKs in intact cell assays [28]. Also, consistent with results from the other RTKs, the 2,4-dichlorophenyl substituent (9) is more potent than the 3,4-dichlorophenyl (4). The most potent inhibitor from this class of compounds contained the dimethoxy substituent (11), and the trimethoxy analog (10) was also an effective inhibitor. Thus, both electron withdrawing and electron donating substituents afforded effective inhibition of IGF1RK.

A second group of inhibitors were the 2-amino-4-anilino-6-phenylethyl pyrrolo[2,3-*d*]pyrimidines (compounds 12–16; Table 2), with an extra methylene unit between the pyrrolo[2,3-*d*]pyrimidine and the benzyl moiety, as compared to compounds 1–11. None of these compounds were effective against IGF1R autophosphorylation, even those with fairly small benzyl groups, such as phenyl (compound 13).

These results suggest that the spacing between the pyrrolo pyrimidine heterocycle and the benzyl group is critical for IGF1R inhibition. The differences between the 6-phenylethyl and 6-phenylmethyl substitutions are currently being explored for selective RTK inhibition.

The 5-substituted 2,4-diaminofuro[2,3-*d*]pyrimidines (compounds 17–19; Table 3) were previously shown to

be effective against a panel of RTKs as well as against dihydrofolate reductase [29]. Both the *E/Z* mixture of 2-naphthyl analogs (17) and the *Z*-isomer (18) were effective against IGF1R autophosphorylation, while the *E*-isomer (19) was ineffective.

One unexpected finding was that two previously reported IGF1R inhibitors, AG538 and AG1024, were ineffective against the isolated IGF1R kinase catalytic domain. While these compounds have not been tested previously against the purified enzyme, they have been shown to be active in both in vitro and in vivo assays [24,25]. AG538 is a substrate-competitive inhibitor with an IC_{50} of 400 nM, as measured in vitro against full-length IGF1R partially purified from CHO cells [24]. AG1024 gave an IC_{50} of 18 μ M against partially purified IGF1R in vitro, and an IC_{50} of 7 μ M against receptor autophosphorylation in intact cells [25]. The lowered effectiveness of these inhibitors against the purified IGF1R kinase domain could be due to the absence of copurifying cellular factors, or to the absence of binding determinants that could be present on the full-length receptor. Additional studies will be needed to distinguish these possibilities. Two other groups of substrate-competitive inhibitors, the cyclo-lignans [33] and catechol isosteres of AG538 [34] also show promise as selective IGF1R inhibitors.

The kinase domains of insulin receptor and IGF1R share 84% amino acid identity [1], and therefore it is not surprising that most of the compounds inhibit the autophosphorylation of both receptors. The maximum selectivity seen in this study (10-fold, for compound 5), does provide some indication that it may be possible to generate inhibitors with a modest degree of selectivity for IGF1R. It may also be possible to generate selectivity by producing compounds that interfere with interactions between IGF1 and its receptor [35]. The selectivity for the unphosphorylated form of IGF1R seen here is a potentially important result because the 2-phenylaminopyrimidine Gleevec (STI-571) effectively inhibits the Bcr-Abl tyrosine kinase by binding to the unphosphorylated form [36]. This suggests that the unphosphorylated forms of tyrosine kinases may be targets for conformation-specific inhibitors.

Acknowledgments

This work was supported by National Institutes of Health Grant CA 28146 to W.T.M.

References

- [1] Ullrich A, Gray A, Tam AW, Yang-Feng T, Tsubokawa M, Collins C, et al. Insulin-like growth factor I receptor primary structure: comparison with insulin receptor suggests structural determinants that define functional specificity. *EMBO J* 1986;5:2503–12.
- [2] Hubbard SR, Till JH. Protein tyrosine kinase structure and function. *Annu Rev Biochem* 2000;69:373–98.

- [3] LeRoith D, McGuinness M, Shemer J, Stannard B, Lanau F, Faria TN, et al. Insulin-like growth factors. *Biol Signals* 1992;1:173–81.
- [4] Adams TE, Epa VC, Garrett TP, Ward CW. Structure and function of the type 1 insulin-like growth factor receptor. *Cell Mol Life Sci* 2000;57:1050–93.
- [5] Baserga R, Hongo A, Rubini M, Prisco M, Valentinis B. The IGF-I receptor in cell growth, transformation and apoptosis. *Biochim Biophys Acta* 1997;1332:F105–26.
- [6] Butler AA, Yakar S, Gewolb IH, Karas M, Okubo Y, LeRoith D. Insulin-like growth factor-I receptor signal transduction: at the interface between physiology and cell biology. *Comp Biochem Physiol B Biochem Mol Biol* 1998;121:19–26.
- [7] Liu JP, Baker J, Perkins AS, Robertson EJ, Efstratiadis A. Mice carrying null mutations of the genes encoding insulin-like growth factor I (Igf-1) and type 1 IGF receptor (Igf1r). *Cell* 1993;75:59–72.
- [8] LeRoith D, Roberts Jr CT. The insulin-like growth factor system and cancer. *Cancer Lett* 2003;195:127–37.
- [9] Valentinis B, Baserga R. IGF-I receptor signalling in transformation and differentiation. *Mol Pathol* 2001;54:133–7.
- [10] Baserga R. The IGF-I receptor in cancer research. *Exp Cell Res* 1999;253:1–6.
- [11] Kaleko M, Rutter WJ, Miller AD. Overexpression of the human insulinlike growth factor I receptor promotes ligand-dependent neoplastic transformation. *Mol Cell Biol* 1990;10:464–73.
- [12] Lu Y, Zi X, Zhao Y, Mascarenhas D, Pollak M. Insulin-like growth factor-I receptor signaling and resistance to trastuzumab (Herceptin). *J Natl Cancer Inst* 2001;93:1852–7.
- [13] LeRoith D, Werner H, Beitner-Johnson D, Roberts Jr CT. Molecular and cellular aspects of the insulin-like growth factor I receptor. *Endocr Rev* 1995;16:143–63.
- [14] Kato H, Faria TN, Stannard B, Roberts Jr CT, LeRoith D. Essential role of tyrosine residues 1131, 1135, and 1136 of the insulin-like growth factor-I (IGF-I) receptor in IGF-I action. *Mol Endocrinol* 1994;8:40–50.
- [15] Munshi S, Kornienko M, Hall DL, Reid JC, Waxman L, Stirdivant SM, et al. Crystal structure of the Apo, unactivated insulin-like growth factor-I receptor kinase. Implication for inhibitor specificity. *J Biol Chem* 2002;277:38797–802.
- [16] Pautsch A, Zoephel A, Ahorn H, Spevak W, Hauptmann R, Nar H. Crystal structure of bisphosphorylated IGF-1 receptor kinase: insight into domain movements upon kinase activation. *Structure (Camb)* 2001;9:955–65.
- [17] Favellyukis S, Till JH, Hubbard SR, Miller WT. Structure and auto-regulation of the insulin-like growth factor 1 receptor kinase. *Nat Struct Biol* 2001;8:1058–63.
- [18] Hubbard SR, Wei L, Ellis L, Hendrickson WA. Crystal structure of the tyrosine kinase domain of the human insulin receptor. *Nature* 1994;372:746–54.
- [19] Hubbard SR. Crystal structure of the activated insulin receptor tyrosine kinase in complex with peptide substrate and ATP analog. *Embo J* 1997;16:5572–81.
- [20] Flores-Riveros JR, Sibley E, Kastelic T, Lane MD. Substrate phosphorylation catalyzed by the insulin receptor tyrosine kinase. Kinetic correlation to autophosphorylation of specific sites in the beta subunit. *J Biol Chem* 1989;264:21557–72.
- [21] Issad T, Tavaré JM, Denton RM. Analysis of insulin receptor phosphorylation sites in intact rat liver cells by two-dimensional phosphopeptide mapping. Predominance of the tris-phosphorylated form of the kinase domain after stimulation by insulin. *Biochem J* 1991;275(Pt 1):15–21.
- [22] Tornqvist HE, Avruch J. Relationship of site-specific beta subunit tyrosine autophosphorylation to insulin activation of the insulin receptor (tyrosine) protein kinase activity. *J Biol Chem* 1988;263:4593–601.
- [23] Wei L, Hubbard SR, Hendrickson WA, Ellis L. Expression, characterization, and crystallization of the catalytic core of the human insulin receptor protein-tyrosine kinase domain. *J Biol Chem* 1995;270:8122–30.
- [24] Blum G, Gazit A, Levitzki A. Substrate competitive inhibitors of IGF-1 receptor kinase. *Biochemistry* 2000;39:15705–12.
- [25] Parrizas M, Gazit A, Levitzki A, Wertheimer E, LeRoith D. Specific inhibition of insulin-like growth factor-I and insulin receptor tyrosine kinase activity and biological function by tyrphostins. *Endocrinology* 1997;138:1427–33.
- [26] Traxler P, Furet P. Strategies toward the design of novel and selective protein tyrosine kinase inhibitors. *Pharmacol Ther* 1999;82:195–206.
- [27] Furet P, Caravatti G, Lydon N, Priestle JP, Sowadski JM, Trinks U, et al. Modelling study of protein kinase inhibitors: binding mode of staurosporine and origin of the selectivity of CGP 52411. *J Comput Aided Mol Des* 1995;9:465–72.
- [28] Gangjee A, Yang J, Ihnat MA, Kamat S. Antiangiogenic and antitumor agents: design, synthesis and evaluation of novel 2-amino-4-(3-bromoanilino)-6-benzylsubstituted Pyrrolo[2,3-*d*]pyrimidines as inhibitors of receptor tyrosine kinases. *Bioorg Med Chem* 2003;11:5155–70.
- [29] Gangjee A, Zeng Y, Ihnat MA, Kamat S, Kisliuk RL. Novel 5-substituted 2,4-diaminofuro[2,3-*d*]pyrimidines as multi-receptor tyrosine kinase and dihydrofolate reductase inhibitors. In: Presented at the American Association for Cancer Research in Washington DC (Abstract Number 3463), 11–14 July 2003.
- [30] Barker SC, Kassel DB, Weigl D, Huang X, Luther MA, Knight WB. Characterization of pp60c-src tyrosine kinase activities using a continuous assay: autoactivation of the enzyme is an intermolecular autophosphorylation process. *Biochemistry* 1995;34:14843–51.
- [31] Yoshimasa Y, Paul JI, Whittaker J, Steiner DF. Effects of amino acid replacements within the tetrabasic cleavage site on the processing of the human insulin receptor precursor expressed in Chinese hamster ovary cells. *J Biol Chem* 1990;265:17230–7.
- [32] Segel IH. Enzyme kinetics: behavior and analysis of rapid equilibrium and steady-state enzyme systems. New York: Wiley; 1975.
- [33] Girmata A, Girmata L, del Prete F, Bartolazzi A, Larsson O, Axelson M. Cyclolignans as inhibitors of the insulin-like growth factor-1 receptor and malignant cell growth. *Cancer Res* 2004;64:236–42.
- [34] Blum G, Gazit A, Levitzki A. Development of new insulin-like growth factor-1 receptor kinase inhibitors using catechol mimics. *J Biol Chem* 2003;278:40442–54.
- [35] Tan C, Wei L, Ottensmeyer FP, Goldfine I, Maddux BA, Yip CC, et al. Structure-based de novo design of ligands using a three-dimensional model of the insulin receptor. *Bioorg Med Chem Lett* 2004;14:1407–10.
- [36] Schindler T, Bornmann W, Pellicena P, Miller WT, Clarkson B, Kuriyan J. Structural mechanism for STI-571 inhibition of abelson tyrosine kinase. *Science* 2000;289:1938–42.